SUPPORTING INFORMATION: Unravelling the hydrophobicity of urea in water using thermodiffusion: implications for protein denaturation

Doreen Niether, Silvia Di Lecce, Fernando Bresme, and Simone Wiegand

October 17, 2017

Contents

1 Refractive index contrast measurements **2**

2 Denaturation of proteins using urea and formamide **3**

3 Density of aqueous urea solutions **5**

4 Concentration scales and conversion for aqueous urea solutions **7**

5 Data from computer simulations **9**
5.1 Comparison of simulation and experiment 9
5.2 Temperature and mole fraction profiles 11
5.3 Soret coefficient and chemical potential 12
5.4 Aggregation of urea molecules 14

1 Refractive index contrast measurements

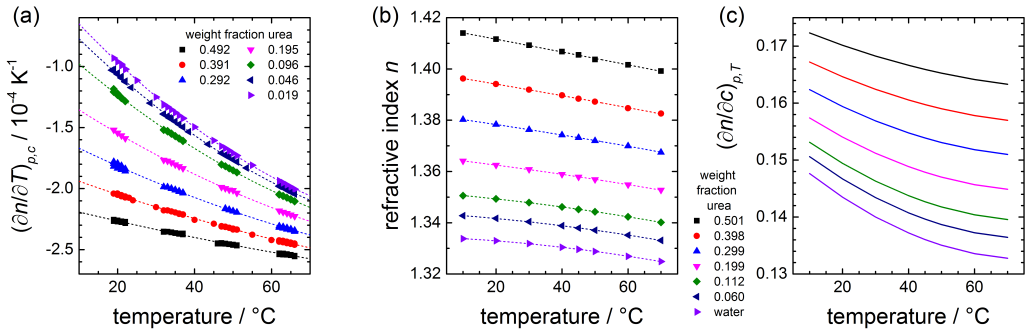


Figure 1: (a) Results of the interferometric measurement of the contrast factor $(\partial n/\partial T)_{p,c}$ for different concentrations of urea in water. (b) Refractive index n for different urea concentrations as a function of temperature. (c) Contrast factor $(\partial n/\partial c)_{p,T}$ calculated from refractive index measurements.

In order to calculate the Soret coefficient S_T from the intensity of the diffracted read-out beam, it is necessary to know the dependence of the refractive index on temperature and concentration, $(\partial n/\partial T)_{p,c}$ and $(\partial n/\partial c)_{p,T}$. The former was measured interferometrically [1] and the latter with an Abbe refractometer (Anton Paar ABBEMAT RXA 158). For the calculation of S_T from the IR-TDFRS measurements, the contrast factors were interpolated from these measurement series for the correct temperatures and concentrations. $(\partial n/\partial T)_{p,c}$ is negative in the measured concentration and temperature range, the absolute value increases with higher urea concentration and with increasing temperature (Fig. 1a). Measurements of the refractive index were conducted for 7 concentrations ranging from pure water ($c = 0$) to an aqueous solution with 50 wt% urea (Fig. 1b). Fig. 1c shows the derivative $(\partial n/\partial c)_{p,T}$ calculated from the function $n(c, T)$ we determined by fitting the experimental values. $(\partial n/\partial c)_{p,T}$ increases at higher urea concentrations and decreases with rising temperature.

2 Denaturation of proteins using urea and formamide

The denaturation of proteins by addition of organic solvents has often been investigated [2, 3, 4, 5, 6, 7, 8, 9, 10]. The question is whether, as in the urea, the denaturation of proteins by formamide occurs in the same concentration range where we observe the changes in the temperature dependent slope of the Soret coefficient in the formamide/water solutions. For formamide (FA) solutions this change occurs for a weight fraction of 0.2 FA corresponding to 4.6 mol/L or a volume fraction of 0.18. Khabiri et al. [9] investigated the influence of formamide 5% (v/v), acetone 20% (v/v) and isopropanol 10% (v/v) on the structure of the haloalkane dehalogenases DhaA, LinB, and DbjA. With the exception of LinB in acetone, the structures of studied enzymes were stabilized in water-miscible organic solvents. The volume fraction of 5% is well below the concentration at which the temperature dependent slope changes, so that we do not expect an effect. Asakura et al. [10] did not observe a denaturation of hemoglobin in the presence of formamide even at very high formamide concentration. Fuchs et al. [7] determine only change of the melting curve. In fig. 2 we see the Soret coefficient as function of concentration. The inversion of the slope can be observed as an 'intersection point', where the T-dependence of S_{T} is close to zero. If we compare the formamide and the urea results, that concentration is w.f. = 0.2 and w.f. = 0.3 for formamide and urea, respectively. In both cases we find a correlation with the denaturation range of the two compounds.

Table 1: UREA

Molarity	weight fraction	reference
4-5	0.23-0.28	[11]
5-6	0.28-0.33	[12]
> 5	> 0.28	[13]
5	0.28	[14]
6	0.33	[15]
5-6	0.28-0.33	[16]
4-6	0.23-0.33	[17]
5.2	0.29	average

Table 2: FORMAMIDE

Molarity	weight fraction	reference
1-2	0.05-0.09	[4]
5.9	0.26	[5]
9.3	0.40	[5]
5-6	0.22-0.26	[8]
4.9	0.21	average

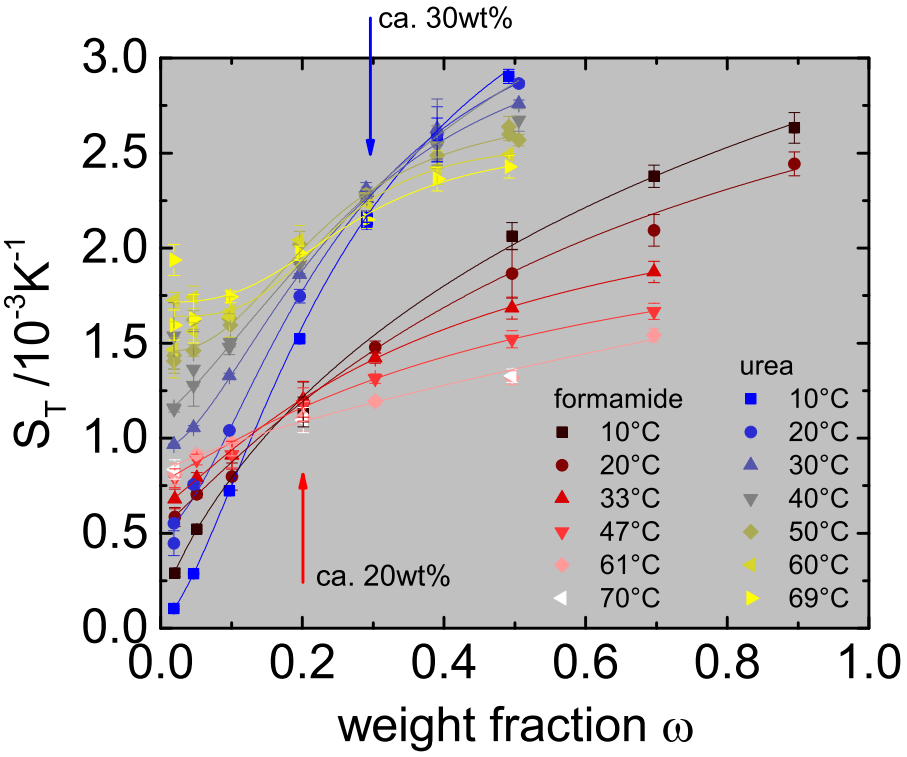


Figure 2: Soret coefficient S_T against concentration for urea and formamide in water. The intersection points at w.f. = 0.3 and w.f. = 0.2 show the concentration where the T-dependence of S_T is inverted.

3 Density of aqueous urea solutions

Densities were measured with an Anton Paar DMA 4500 densimeter with an error of 0.0002 g/cm^3. Solutions were prepared with Urea ($\geq$ 99%, Fluka, Sigma-Aldrich, 89555 Steinheim, Germany) and Millipore water. For degassing, the sample solutions were sealed in their flasks with Parafilm and kept in an ultra-sonic bath at 70°C for 2h. No formation of bubbles was observed during the measurements, except for the 5 wt% solution at 60 and 65°C.

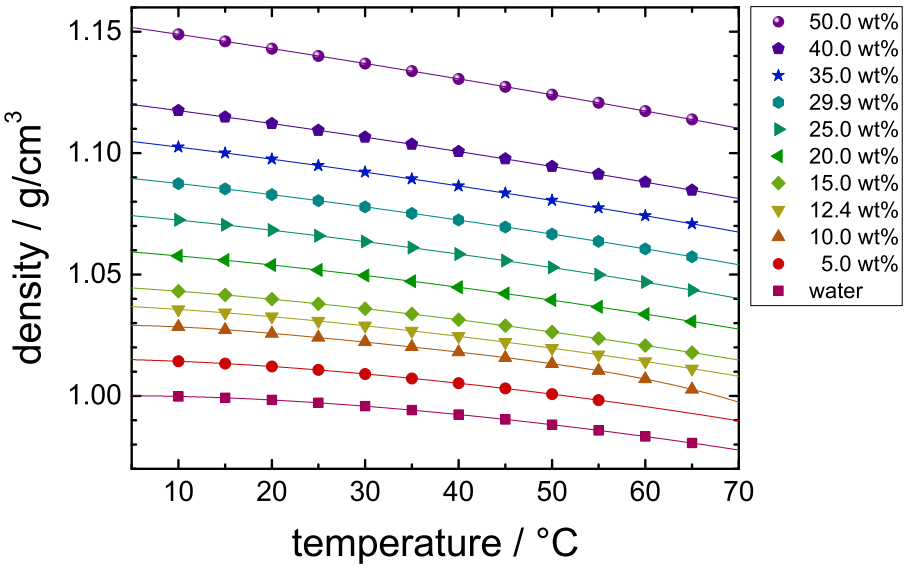


Figure 3: Density ρ against temperature for the measured urea solutions and water. Values can also be found in Table 3.

The following empirical equation (1) was found by fitting the experimental data and can be used to interpolate the temperature and concentration dependant density of aqueous urea solutions. Note that the units of ρ, ω, and T are g/cm^3, weight fractions, and °C, respectively.

$$\rho(\omega, \mathrm{T}) = (0.99965{+}0.30714{\cdot}\omega){+}(5.92438{\cdot}10^{-5}{-}0.00187{\cdot}\omega{+}0.00141{\cdot}\omega^2){\cdot}\mathrm{T}{+} (-8.31302 \cdot 10^{-6} + 2.38684 \cdot 10^{-5} \cdot \omega - 2.5325 \cdot 10^{-5} \cdot \omega^2) \cdot \mathrm{T}^2{+} (5.34609{\cdot}10^{-8}{-}7.13453{\cdot}10^{-8}{\cdot}\omega){\cdot}\mathrm{T}^3{+}(-2.52222{\cdot}10^{-10}{+}2.08659{\cdot}10^{-10}{\cdot}\omega){\cdot}\mathrm{T}^4 \quad (1)$$

Table 3: Measurement results for the density ρ of aqueous urea solutions with weight fractions of urea from w.f. = 0 to w.f. = 0.5 and at temperatures between 10 and 65°C.

w.f.	ρ / g/cm^3					
	10°C	15°C	20°C	25°C	30°C	35°C
0	0.9998	0.9992	0.9983	0.9972	0.9958	0.9942
0.0503	1.0143	1.0133	1.0121	1.0107	1.0091	1.0072
0.0997	1.0285	1.0272	1.0257	1.0241	1.0222	1.0202
0.1242	1.0356	1.0343	1.0326	1.0309	1.0289	1.0268
0.1497	1.0431	1.0416	1.0399	1.0380	1.0359	1.0337
0.1999	1.0577	1.0559	1.0539	1.0518	1.0496	1.0472
0.2497	1.0724	1.0704	1.0682	1.0660	1.0635	1.0610
0.2991	1.0875	1.0853	1.0829	1.0804	1.0779	1.0752
0.3500	1.1025	1.1001	1.0975	1.0949	1.0922	1.0894
0.4001	1.1175	1.1149	1.1122	1.1094	1.1066	1.1036
0.5001	1.1489	1.1460	1.1430	1.1400	1.1369	1.1338
	40°C	45°C	50°C	55°C	60°C	65°C
0	0.9924	0.9903	0.9882	0.9858	0.9833	0.9806
0.0503	1.0053	1.0031	1.0008	0.9983	–	–
0.0997	1.0180	1.0157	1.0133	1.0104	1.0070	1.0027
0.1242	1.0246	1.0222	1.0196	1.0170	1.0142	1.0112
0.1497	1.0314	1.0289	1.0263	1.0236	1.0208	1.0179
0.1999	1.0448	1.0422	1.0394	1.0366	1.0337	1.0307
0.2497	1.0584	1.0557	1.0529	1.0499	1.0468	1.0436
0.2991	1.0724	1.0696	1.0667	1.0637	1.0605	1.0574
0.3500	1.0865	1.0835	1.0805	1.0774	1.0742	1.0709
0.4001	1.1007	1.0976	1.0945	1.0913	1.0880	1.0847
0.5001	1.1306	1.1273	1.1241	1.1207	1.1173	1.1138

4 Concentration scales and conversion for aqueous urea solutions

The weight fraction of urea ω_{urea} is the ratio of the mass of urea m_{urea} and the total mass of the solution $(m_{urea} + m_{water})$:

$$\omega_{urea} = m_{urea}/(m_{urea} + m_{water}) \tag{2}$$

The mole fraction of urea χ_{urea} is defined as the ratio of the number of urea molecules N_{urea} and the total number of molecules $(N_{urea} + N_{water})$:

$$\chi_{urea} = N_{urea}/(N_{urea} + N_{water}) \tag{3}$$

With $N = m/M$, $\omega_{water} = 1 - \omega_{urea}$, and the molar masses for urea and water, M_{urea} =60.05526 g/mol and M_{water} =18.01528 g/mol, mole fractions can be calculated with

$$\chi_{urea} = (\omega_{urea}/M_{urea})/[(\omega_{urea}/M_{urea}) + (\omega_{water}/M_{water})]. \tag{4}$$

The number of water molecules per urea molecule can be calculated from χ with $N_{urea} = 1$ and

$$N_{water} = (N_{urea}/\chi_{urea}) - N_{urea}. \tag{5}$$

The molar concentration c is defined as the number of urea molecules in the volume of the solute

$$c_{urea} = N_{urea}/V, \tag{6}$$

where the volume V is given by

$$V = (m_{urea} + m_{water})/\rho. \tag{7}$$

In our case, where the density ρ is given in g/cm^3, c in the unit M = mol/L can be calculated from ω with

$$c_{urea} = (\omega_{urea}/M_{urea}) \cdot \rho \cdot 1000. \tag{8}$$

Note that the maximal value for the molar concentration at a mole fraction of $\chi_{urea} = 1$ is calculated as c_{urea} =21.56 M, which, considering that the density used for the calculation is extrapolated from the aqueous solution, is in reasonable agreement with the value of 21.98 M calculated for pure solid urea with a density of $\rho_{urea} = 1.32$ g/cm^3.

Table 4: Conversion table for concentrations of aqueous urea solutions in weight fraction ω, mole fraction χ, molar concentration c and molecular ratio urea:water in a concentration range from $\omega = 0$ to $\omega = 0.5$.

χ	ω	c / M	urea:water		ω	χ	c / M	urea:water
0.01	0.03258	0.54622	1:99		0.05	0.01554	0.84306	1:63.34
0.05	0.14926	2.58461	1:19		0.1	0.03226	1.70936	1:30
0.1	0.27028	4.83616	1:9		0.2	0.06976	3.51320	1:13.33
0.15	0.37039	6.80652	1:5.67		0.3	0.11392	5.41460	1:7.78
0.2	0.45456	8.54050	1:4		0.4	0.16666	7.41662	1:5
0.25	0.52633	10.07544	1:3		0.5	0.23076	9.52234	1:3.33
c / M	χ	ω	urea:water		c / M	χ	ω	urea:water
1	0.0185	0.0592	1:53.01		6	0.1286	0.3298	1:6.77
2	0.0381	0.1165	1:25.28		7	0.1551	0.3796	1:5.45
3	0.0587	0.1721	1:16.04		8	0.1834	0.4282	1:4.45
4	0.0806	0.2261	1:11.41		9	0.2139	0.4757	1:3.67
5	0.1039	0.2787	1:8.63		10	0.2468	0.5221	1:3.05

5 Data from computer simulations

5.1 Comparison of simulation and experiment

To test the accuracy of our forcefields for urea-water solutions we performed a number of simulations and computed the density and diffusion coefficient as a function of urea concentration. Figure 4 shows the concentration dependence of the density with urea concentration at 25^0C. Both experiments and simulations shows an increase of the solution density with the urea concentration. Our computed values are in excellent agreement with both experimental [18] and simulated [19] results obtained at the same thermodynamic state, in the latter case using a different force-field.

Figure 5 shows the diffusion coefficient D for several concentrations as a function of temperature. The simulation data for the diffusion coefficient were calculated using equilibrium simulations ensemble and via the mean square displacement and Einstein equation [20].

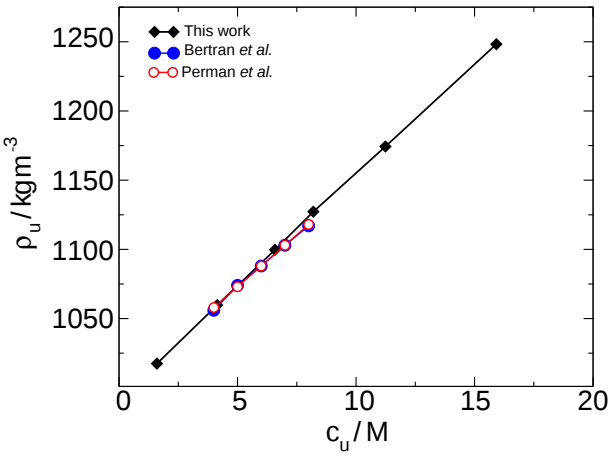


Figure 4: Concentration dependence of density for urea solutions at 25^0C. The simulation results are compared with both experimental [18] and simulation [19] data using a different forcefield. All the data correspond to the same thermodynamic state.

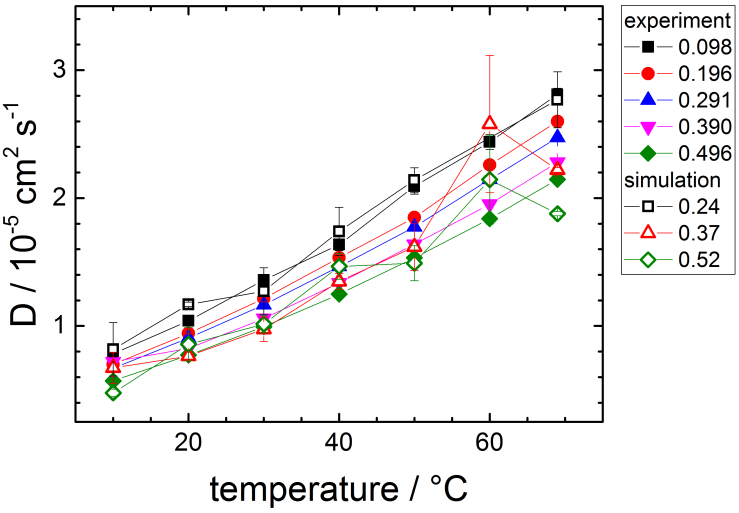


Figure 5: Diffusion coefficient D against temperature for different concentrations from IR-TDFRS measurements (lines) and simulations (symbols).

5.2 Temperature and mole fraction profiles

In order to compute the Soret coefficient we performed Non-Equilibrium Molecular Dynamics (NEMD) simulations as described in the Methods section.

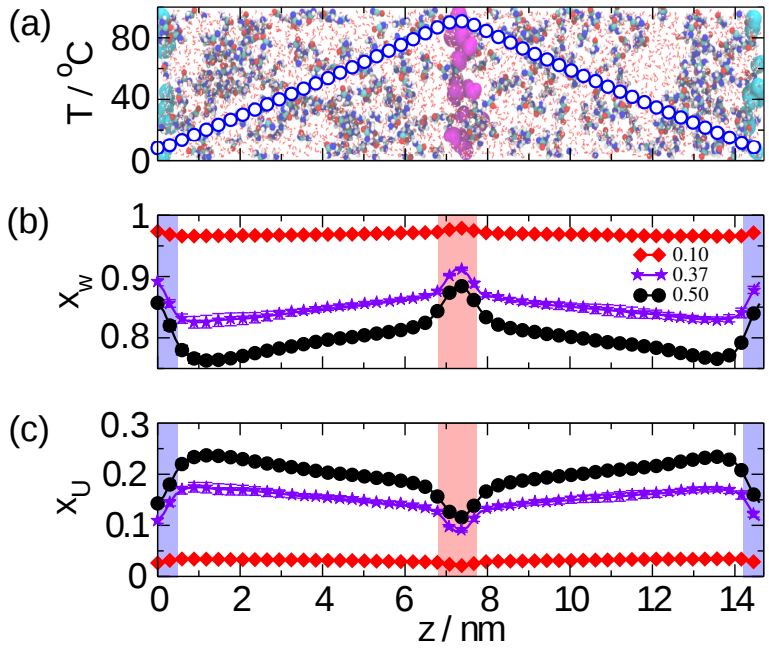


Figure 6: Temperature profile (a) water mole fraction (b) and urea mole fraction (c) along the simulated box for different urea concentrations. The red and blue squares in panel (b) and (c) indicate the position of the hot and cold thermostatted layers, respectively.

Figure 6 (a) show a typical snapshot of the system simulated in this work, along with a representative temperature profile. The hot and cold thermostatted molecules are represented in magenta and cyan, respectively. The temperatures in the cold and hot layers were set to 2^0C and 102^0C, respectively, and result in a well defined temperature profile along the simulated box. The size of the water molecules, in red, was decreases to allow a better visualization of the urea molecules. Figure 6 (b) and (c) shows the mole fraction of water and urea, respectively, for different urea concentrations. Both, the mole fraction of urea and water changes along the simulated box and with temperature as a results of the thermal gradient applied. The data were acquired at the stationary state, *i.e* when there is no net mass flux. The variation in mole fraction along the simulated box was used to compute the Soret coefficient (see equation (4) in the Methods section). We neglected

the data next to the thermostatted layers.

5.3 Soret coefficient and chemical potential

Table 5 shows the computed Soret coefficient values for the three concentrations considered in this work (concentrations 10 wt% (1.7 M), 37 wt% (6.7 M) and 50 wt% (9.4 M), shown in fig. 1b of the main text), along with the fitting parameters used to model our data using the Iacopini and Piazza equation [21] (equation 2 in the main text) or the expression $S_{\mathrm{T}} = S_{\mathrm{T}}^{\infty} + S_{\mathrm{T}}^{0} \cdot \exp(-T/T_0)$ in case of negative temperature dependence (0.50 - U1). The labels U1 and U2 in the table, indicate the different water-urea interactions used in this work (see the main text for more details). The chemical potential of urea was computed as described in the Methods section and then fitted to a linear equation ($\mu_{tot}(T) = mT + q$) to calculate the entropy and enthalpy. The fitting parameters are reported in the last column of Table 5. The fitting of the chemical potential was obtained using the Kelvin scale, while that one for the Soret coefficient using the Celsius scale. Note that the values of the Soret coefficient are independent on the scale used.

Table 5: Soret coefficient S_T for different concentrations of water computed via NEMD simulations. In order to describe the temperature dependence of S_T the adjustable parameter sets S_T^∞, T^* and T_0 or S_T^∞, S_T^0 and T_0 are used. Additionally the adjustable parameters m and q are listed to describe the temperature dependence of the chemical potential of urea in the water-urea solutions.

conc. $w.f.$	T / °C	S_T / $10^{-3}K^{-1}$	S_T^∞ / $10^{-3}°C^{-1}$	T^* / °C	T_0 / °C
0.1	29.63	0.236 ± 0.358	4.632	29.437	22.765
	40.01	0.966 ± 0.229			
	50.28	3.624 ± 0.386			
	60.52	3.326 ± 0.379			
	70.85	3.719 ± 0.391			
0.37	22.52	2.925 ± 0.332	4.588	15.734	6.6907
	34.48	4.296 ± 0.487			
	46.64	4.625 ± 0.539			
	59.11	4.380 ± 0.516			
	72.01	4.718 ± 0.596			
0.50 – U2	27.24	2.006 ± 0.194	3.065	16.102	10.3838
	38.09	2.826 ± 0.300			
	48.93	2.881 ± 0.213			
	59.96	2.872 ± 0.220			
	71.27	3.246 ± 0.252			

			S_T^∞ / $10^{-3}°C^{-1}$	S_T^0 / $10^{-3}°C^{-1}$	T_0 / °C
0.50 – U1	26.66	6.435 ± 0.711	3.676	8.753	23.4695
	37.28	5.571 ± 0.624			
	48.07	4.938 ± 0.561			
	59.10	3.948 ± 0.464			
	70.41	4.354 ± 0.526			

conc. $w.f.$			m / kJmol^{-1} K^{-1}	q / kJmol^{-1}
0.1			0.112	−73.624
0.37			0.136	−78.071
0.50 – U1			0.139	−78.522
0.50 – U2			0.142	−82.505

5.4 Aggregation of urea molecules

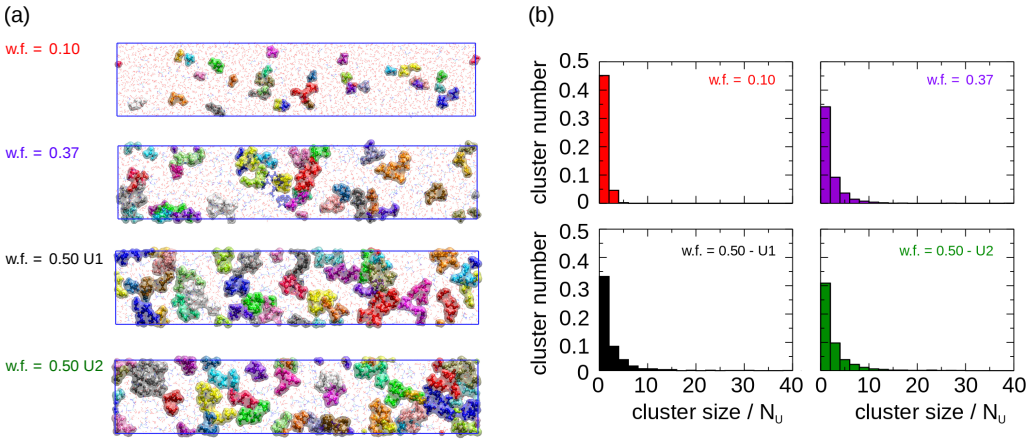


Figure 7: (a) Snapshot of urea water mixture showing the aggregation of urea molecules at different concentrations. Clusters with different size are represented with different colors. (b) Cluster size distribution computed through the average of 100 configuration over 15 ns.

To explain the thermodiffusive behaviour of the aqueous urea solutions we quantified the clustering of urea molecules. We performed a 3D Voronoi tessellation of the solutions at 30^0C using the voro++ package [22]. Each urea molecule has been represented according to the position of the C=O group which has been considered as the center of the molecule to construct the cluster.

Figure 7 illustrates the urea aggregation as a function of the urea concentration. In the snapshots on the left side of Figure 7 (a), clusters with different size are represented with different colors. Water and urea molecules not aggregated are represented with lines. Urea molecules aggregate creating an amount of clusters which increases, as well as their size, with concentration. Furthermore, we show, in Figure 7 (b), the cluster size distribution representing the normalized number of clusters against the cluster size, in terms of number of urea molecules, N_U. This graphical representation of the numerical data was obtained by computing the average cluster number and size of 100 configurations over 15 ns. At the highest concentration considered, 50 wt%, we find that the increase in water-urea interactions (U2) results in a decrease of both the size and number of cluster. Indeed, we quantified the aggregation by computing the mean size of the clusters, $< S_{U,cluster} >$, using:

$$< S_{U,cluster} >= \int_{s_{min}}^{s_{max}} s n_s(s) ds, \tag{9}$$

where $n_s(s)$ represent the number of cluster with size s, and s_{min} and s_{max} are the lowest and highest cluster size observed for these simulated systems, respectively.

Table 6: Mean size of the clusters, $< S_{U,cluster} >$ as a function of different weight fractions and water-urea interactions.

force field	$w.f.$	$< S_{U,cluster} > / N_u$
U1	0.10	2.20
U1	0.37	3.16
U1	0.50	4.83
U2	0.50	3.76

Table 5 shows the mean size of the clusters, $< S_{U,cluster} >$ for the different simulated systems. $< S_{U,cluster} >$ decreases with the increase of the water-urea interaction (see w.f. = 0.5 U1 and U2), loosing about one urea molecule per cluster and being closer to the cluster size obtained at lower concentration, namely w.f. = 0.37. At this concentration the Soret coefficient increases with temperature. We find that the increase in the water-urea interactions results in a reduction of clustering, hence better solubility in water, which correlates well with our hypothesis that stronger solvation leads to a less thermophobic state.

References

[1] A. Becker, W. Köhler, and B. Müller. *Ber. Bunsen. Phys. Chem.*, 99(4):600–608, 1995.

[2] T. Samejima and K. Shibata. *Archives of Biochemistry and Biophysics*, 93:407, 1961.

[3] L. Casiraghi G. Invernizzi, R. Grandori, and M. Lotti. *Journal of Biotechnology*, 141:42–46, 2009.

[4] R. D. Blake and S. G. Delcourt. *Nucleic Acids Research*, 24:2095–2103, 1996.

[5] Y. L. Khmelnitsky, V. V. Mozhaev, A. B. Belova, M. V. Sergeeva, and K. Martinek. *European Journal of Biochemistry*, 198:31–41, 1991.

[6] C. Tibbetts, K. Johansson, and L. Philipson. *Journal of Virology*, 12:218–225, 1973.

[7] J. Fuchs, D. Dell'Atti, A. Buhot, R. Calemczuk, M. Mascini, and T. Livache. *Analytical Biochemistry*, 397:132–134, 2010.

[8] L. S. Yilmaz, A. Loy, E. S. Wright, M. Wagner, and D. R. Noguera. *Plos One*, 7(8), 2012.

[9] M. Khabiri, B. Minofar, J. Brezovsky, J. Damborsky, and R. Ettrich. *Journal of Molecular Modeling*, 19:4701–4711, 2013.

[10] T. Asakura, K. Adachi, and E. Schwartz. *Journal of Biological Chemistry*, 253:6423–6425, 1978.

[11] M. C. Stumpe and H. Grubmüller. *J. Phys. Chem. B*, 111:6220–6228, 2007.

[12] N. Samanta, D. Das Mahanta, and R. K. Mitra. *Chemistry-an Asian Journal*, 9:3457–3463, 2014.

[13] L. B. Sagle, Y. J. Zhang, V. A. Litosh, X. Chen, Y. Cho, and P. S. Cremer. *J. Am. Chem. Soc.*, 131:9304–9310, 2009.

[14] A. Idrissi, M. Gerard, P. Damay, M. Kiselev, Y. Puhovsky, E. Cinar, P. Lagant, and G. Vergoten. *J. Phys. Chem. B*, 114:4731–4738, 2010.

[15] Y. Hayashi, Y. Katsumoto, S. Omori, N. Kishii, and A. Yasuda. *J. Phys. Chem. B*, 111:1076–1080, 2007.

[16] D. Bandyopadhyay, S. Mohan, S. K. Ghosh, and N. Choudhury. *J. Phys. Chem. B*, 118:11757–11768, 2014.

[17] A. Tischer and M. Auton. *Protein Science*, 22:1147, 2013.

[18] Edgar Philip Perman and Trevor Lovett. *Trans. Faraday Soc.*, 22:1–19, 1926.

[19] Celso A. Bertran, José J. V. Cirino, and Luiz C. G. Freitas. *J. Braz. Chem. Soc.*, 13:238 – 244, 00 2002.

[20] M.P. Allen and D.J. Tildesley. *Computer Simulation of Liquids*. Oxford Science Publ. Clarendon Press, 1989.

[21] S. Iacopini and R. Piazza. *Europhys. Lett.*, 63:247–253, 2003.

[22] Chris H. Rycroft. *Chaos*, 19:041111, 2009.